Fluctuation of long-range order in Co-Pt alloy nanoparticles revealed by time-resolved electron microscopy

Kazuhisa Sato and Hidehiro Yasuda

Citation: Appl. Phys. Lett. **110**, 153101 (2017); doi: 10.1063/1.4980077
View online: http://dx.doi.org/10.1063/1.4980077
View Table of Contents: http://aip.scitation.org/toc/apl/110/15
Published by the American Institute of Physics

Fluctuation of long-range order in Co-Pt alloy nanoparticles revealed by time-resolved electron microscopy

Kazuhisa Sato[1] and Hidehiro Yasuda[1,2]
[1]*Research Center for Ultra-High Voltage Electron Microscopy, Osaka University, Ibaraki, Osaka 567-0047, Japan*
[2]*Division of Materials and Manufacturing Science, Graduate School of Engineering, Osaka University, 2-1 Yamadaoka, Suita, Osaka 565-0871, Japan*

(Received 9 February 2017; accepted 31 March 2017; published online 10 April 2017)

The development of long-range order in disordered Co-Pt alloy nanoparticles has been atomically resolved *in situ* with an ultra-high voltage electron microscope equipped with a direct electron detection camera. Electron-irradiation-enhanced ordering occurred at 573 K with 1 MeV electrons at a dose rate of 8.9×10^{24} e/m^{2}s. High-speed (400 frames/s) imaging revealed fluctuations of the c-axis orientation of the $L1_0$–type ordered structure. Specifically, the c-axis orientation changes occurred at 2.5-ms intervals. Thus, the atomic ordering rate at 573 K is deduced to be 3×10^{-17} m^2/s, which is 10^{13} times higher than that estimated for interdiffusion in a bulk Co-Pt alloy. The observed kinetic ordering temperature of 573 K is significantly lower than that reported previously (>800 K). The low-temperature ordering may be the result of enhanced atom migration via excess vacancies, 10^6 times higher than that at thermal equilibrium, introduced by the high-energy electron irradiation. *Published by AIP Publishing.* [http://dx.doi.org/10.1063/1.4980077]

Recent demands for ultrahigh density magnetic storage require recording media with high magnetocrystalline anisotropy energy (MAE) to ensure the thermal stability of magnetization. Equiatomic Co-Pt alloy nanoparticles (NPs) are candidate materials because of their hard magnetic properties attributed to the tetragonal $L1_0$-type ordered structure.[1] The MAE is dependent on the degree of order in the ordered structure, and therefore, formation of the ordered phase in small NPs is a key issue for practical applications.[2] So far, there have been several attempts to directly observe atomic ordering using *in situ* transmission electron microscopy (TEM).[3–6] However, as the temperature is increased, cooperative atomic ordering proceeds so rapidly that it has not been imaged with a conventional TV-rate camera (30 frames/s (fps)).[6] Direct electron detection cameras (DDCs) overcome this limit with frame rates exceeding 400 fps. Temperature-dependent atomic ordering can be enhanced by electron irradiation.[7–13] Triggering atomic ordering is easier to control by electron irradiation than by temperature changes. Here, we observe disorder-order transition of Co-Pt NPs with atomic resolution by using an ultra-high voltage electron microscope (UHVEM) equipped with a DDC.

Thin films of disordered Co-Pt alloy NPs were fabricated by co-deposition of Co (99.98%) and Pt (99.95%) targets via rf-magnetron sputtering onto NaCl(001) substrates kept at 620 K. After the co-sputtering of Co and Pt, the surface of the NPs was coated by amorphous carbon (a-C) thin films. The sputtering was performed at 10 mtorr of Ar gas (99.999%) in a chamber having a base pressure of 2×10^{-6} Pa. Sputtering powers were 80 and 45 W for Co-Pt and C, respectively. The films were removed from the NaCl substrate by immersion in distilled water; the floating films were then mounted onto molybdenum TEM micro-grids. Structures and compositions of the NPs were characterized with a JEOL JEM-ARM200F TEM operating at 200 kV and equipped with an energy dispersive x-ray spectrometer (EDS). Electron irradiation and simultaneous *in situ* observation were performed with a JEOL JEM-1000EES UHVEM operating at 1 MV equipped with a DDC (Gatan K2 IS) and a charge-coupled device (CCD) camera (Gatan Orius SC200D). The nominal point resolution of the UHVEM is 0.16 nm at 1 MV. The dose rate was adjusted with the condenser lens current in the TEM mode and measured with a Faraday cage attached to the UHVEM.

Figure 1 shows a selected area electron diffraction (SAED) pattern and a TEM image of as-sputtered Co-Pt alloy NPs with the disordered fcc structure; the image was acquired with the CCD camera attached to the UHVEM. The (001)-oriented, 10-nm-sized Co-Pt alloy NPs are dispersed. The average alloy composition of Co-45 at. % Pt was determined by EDS analysis, assuming the thin film approximation. To obtain the

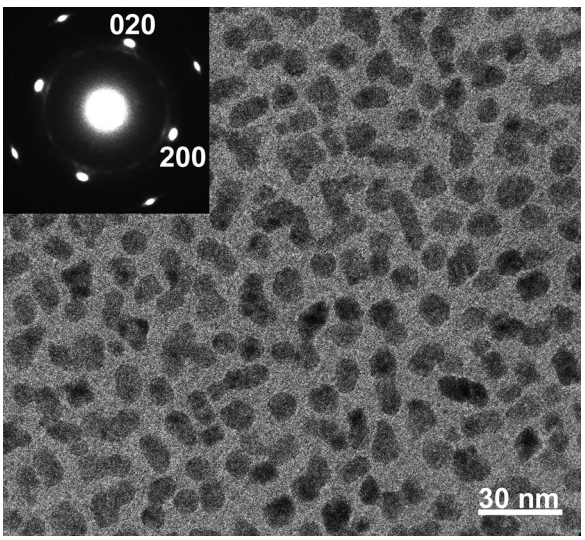

FIG. 1. SAED pattern (upper left corner) and a TEM image of as-sputtered Co-45 at. % Pt alloy NPs with the disordered fcc structure.

$L1_0$ ordered phase, post-deposition annealing is necessary; it was previously shown that the kinetic ordering temperature for sputtered Co-Pt alloy NPs is 800 K.[14]

Figure 2 shows continuous TEM images of a Co-Pt alloy NP acquired at 400 fps (2.5 ms/frame) with the K2 IS DDC. Fast Fourier transform (FFT) patterns of the entire NP are shown in the lower right of each image. The image size is 1920×1792 pixels with the pixel size of 0.022 nm. The observation was made at 573 K under 1 MeV electron irradiation at a dose rate of 8.9×10^{24} e/m^{2}s (8.9×10^{6} e/nm^{2}s). Atomic ordering was detected at a total dose of approximately 1×10^{26} e/m^2 (~10 s of electron irradiation), which may correspond to the critical total dose for a structural transition in a small NP. Reuter *et al*. reported a similar total dose for atomic ordering in an Fe-50 wt. % Ni alloy. They observed superlattice reflections at 583 K after 1 MeV electron irradiation at a total dose of 3.6×10^{26} e/m^2 (6×10^{24} e/m^{2}s for 60 s).[13]

In Fig. 2(a), crossed {200} lattice fringes indicate a chemically disordered NP with the face-centered cubic (fcc) structure. After 2.5 ms, ordered fringes appear in Fig. 2(b). The 3–5-nm local ordered regions (encircled areas) are characterized by (001) lattice fringes. The orientation of the crystallographic c-axis is indicated in the image. The atomic ordering was also confirmed by the appearance of 001 superlattice reflections in the attached FFT patterns for each ordered area in the NP. After another 2.5 ms [Fig. 2(c)], the c-axis in the local ordered region rotated 90° in the film plane. In Fig. 2(d), the ordered phase disappeared, and then re-appeared in Figs. 2(e) and 2(f). An ordered domain with the c-axis oriented normal to the film plane (c-domain) was not observed in these images. This can be attributed to a probability issue on variant selection because the frequency was extremely low: only 12 of 1000 successive TEM images had c-domains, unlike the case of atomic ordering by annealing.[3,14,15]

The above observations are not the result of defocus instabilities of the objective lens because the high-voltage stability is $<8 \times 10^{-7}$/min at 1 MV. Crystal tilt and particle thickness affect high-resolution TEM imaging of NPs,[16] but these can be ruled out in this study by the experimental results and image simulations. A possible temperature rise during electron irradiation was estimated using the method reported by Jenčič *et al*., which assumes a homogeneous sample and differs from the granular sample here.[17] The obtained value is less than 1 K, and hence, it is practically negligible. Evidence that a temperature rise was negligible is that during the *in situ* observations, the lattice parameter deduced from the FFT patterns of an irradiated NP was constant, and there was no specimen drift.

Thus, it can be concluded that fluctuations of the c-axis orientation were observed during the early stages of atomic ordering. Similar results were obtained for ten NPs. The signal-to-noise ratio for each image was low because of the high frame rate; however, atomic ordering can be confirmed based on lattice fringes together with FFT patterns. In the latter, the peak-to-background ratio for the 002 fundamental reflection and the 001 superlattice reflection were

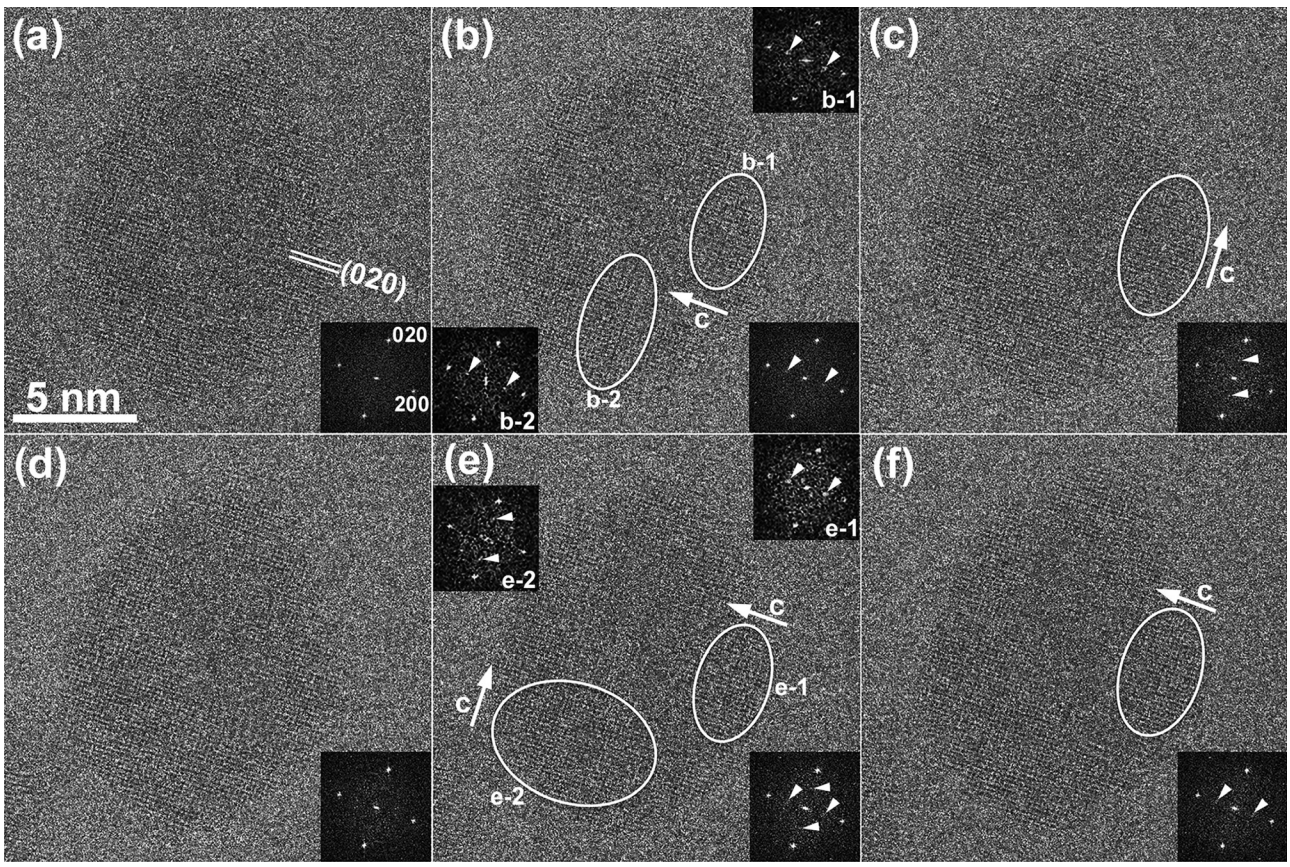

FIG. 2. TEM images of a Co-Pt alloy NP acquired at 400 fps (2.5 ms/frame). Atomic ordering was detected after electron irradiation at a total dose of approximately 1×10^{26} e/m^2. (b) and (e) include separate FFTs for two types of ordered domains.

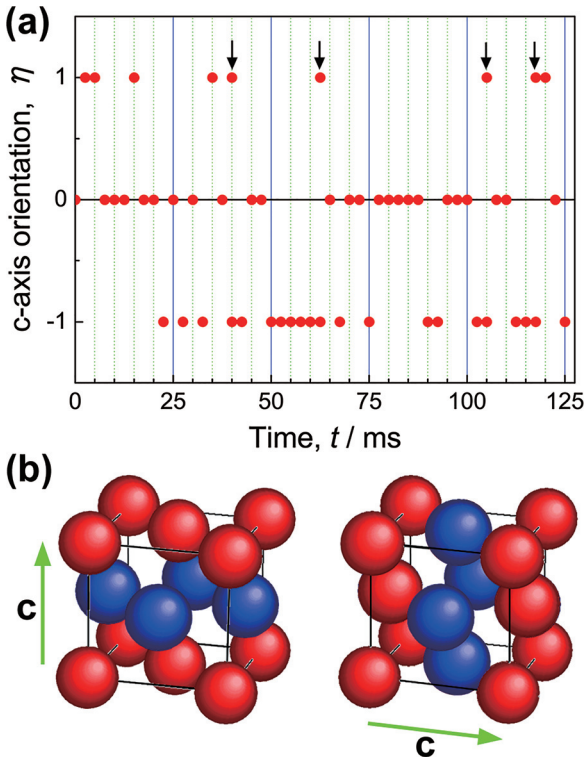

FIG. 3. (a) Fluctuation of the c-axis orientation as detected by lattice images and corresponding FFT patterns obtained every 2.5 ms. In the vertical axis, $\eta = \pm 1$ denotes long-range order with the c-axis oriented parallel to [100] and [010] of the disordered phase, respectively, while $\eta = 0$ denotes the disordered state. (b) Schematics of the $L1_0$-type ordered structure.

estimated to be 1.36 ± 0.07 and 1.18 ± 0.03, respectively. Hence, the appearance of the superlattice reflection is statistically significant.

Figure 3 (a) plots the variation in c-axis orientation as a function of time over 2.5-ms intervals for the entire NP shown in Fig. 2. Along the vertical axis, $\eta = \pm 1$ indicates long-range order with the c-axis oriented parallel to [100] and [010] of the disordered phase, respectively, while $\eta = 0$ refers to the disordered state. Arrows indicate the coexistence of two types of ordered domains with orthogonal c-axis orientations, which suggests that any one of the three $\langle 100 \rangle$ axes of the Co-Pt disordered phase could act as the c-axis of the tetragonal ordered structure.[18] This result also indicates that ordered nanoscale domains can coexist in a NP, as previously reported.[18,19] High-speed images revealed fluctuations of the c-axis orientation in the $L1_0$ ordered structure. Replacement of nearest neighbor atoms via a vacancy can cause variation of local atomic order in the $L1_0$-type ordered structure, as shown in Fig. 3(b). Thus, long-range atom migration is not necessary for atomic ordering or rotation of the c-axis. Such an exchange of nearest neighbor atoms occurred at 573 K within 2.5 ms. Hence, the atom diffusivity was deduced to be 3×10^{-17} m^2/s at 573 K under 1 MeV electron irradiation. This is 10^{13} times higher than a value at 573 K, estimated with a frequency factor and activation energy for interdiffusion in a bulk Co-50 at. % Pt alloy.[20]

The high effective diffusivity corresponds to a value expected at 1160 K, which is just above the order-disorder transition temperature of a bulk alloy. A vacancy concentration C_v can be estimated from $C_v = \exp(S_f/k_B)\exp(-E_f/k_BT)$,

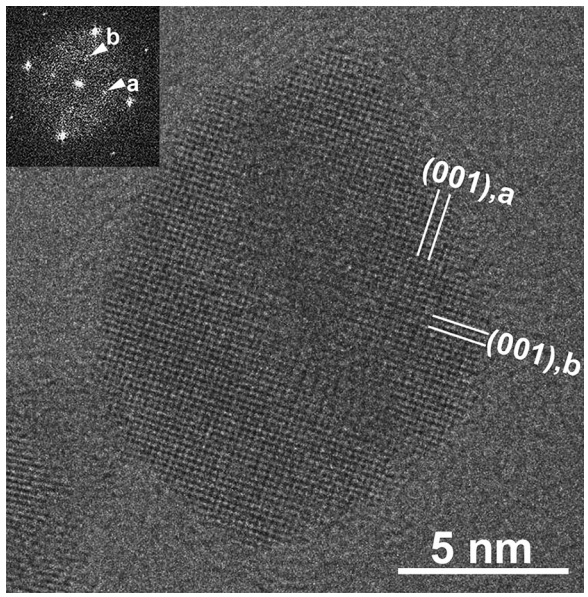

FIG. 4. Composite TEM image integrating the six images shown in Figs. 2(a) to 2(f). Arrowheads labeled as "a" and "b" indicate two types of orthogonal 001 superlattice reflections from the a- and b-domains.

where S_f is the formation entropy of a vacancy, E_f the formation energy of a vacancy, k_B the Boltzmann constant, and T the temperature. From this relation, C_v at 573 K under 1 MeV electron irradiation (equivalent to the value at 1160 K) is $\sim 10^6$ times higher than that at thermal equilibrium at 573 K, assuming $S_f \sim 1.5 k_B$ and $E_f \sim 1.5$ eV.[21,22] The effective diffusivity is even higher than that reported for the crystallization of amorphous alloys (10^{-20}–10^{-18} m^2/s).[23] This high mobility of atoms is derived from a different mechanism rather than from bulk diffusion by heat treatment.

Figure 4 shows a composite TEM image integrating the six consecutive images in Figs. 2(a) to 2(f). Two orthogonal ordered domains with c-axes oriented in-plane (a- and b-domains) are seen in the image due to integration of events occurred within 12.5 ms, in contrast to the time-resolved observation. The attached FFT pattern includes two different orthogonal 001 superlattice reflections (marked as "a" and "b") that arose from the a- and b-domains. The image contrast is somewhat blurred in the center of the NP, which may be produced by an intermediate stage of ordering such as formation of a domain boundary. Unlike a TV-rate camera, the 2.5-ms-time-resolved TEM observations can detect the fluctuation of c-axis orientation.

The observed kinetic ordering temperature of 573 K for binary CoPt NPs is significantly lower than that reported previously (>800 K).[14] The displacement threshold energies for Co and Pt are 22 and 33 eV, respectively.[24,25] On the other hand, the maximum transfer energy of a 1 MeV electron can be calculated to be 74 eV for Co and 22 eV for Pt.[26] From the displacement threshold energies and the McKinley-Feshbach equation,[27] the threshold voltages are 0.42 MV (Co) and 1.3 MV (Pt). Therefore, with respect to the cross sections of atomic displacements, a knock-on displacement of Co atoms in the Co-Pt alloy is dominant under 1 MeV electron irradiation. The formation of vacancies and interstitial atoms induces disordering, while energy-dissipative processes enhance atomic ordering. The

dominant process varies depending on the irradiation temperature. Schulson concluded that thermally activated migration of irradiation-produced vacancies is the dominant ordering mechanism during electron irradiation.[8] Thus, the observed low temperature atomic ordering by high-energy electron irradiation can be attributed to enhanced atom migration via excess vacancies, which have a concentration more than $\sim 10^6$ times than that for thermal equilibrium.

In summary, we have observed atomic ordering of Co-Pt alloy NPs using a UHVEM equipped with a DDC. The electron-irradiation-enhanced ordering occurred at 573 K under 1 MeV electron irradiation at a dose rate of 8.9×10^{24} e/m^{2}s. Fluctuations of the c-axis orientation were detected at a 2.5-ms timescale during the early stages of atomic ordering. This cannot be resolved by conventional *in-situ* TEM observation using a TV-rate camera. The high mobility of atoms (3×10^{-17} m^2/s) was deduced assuming the replacement of nearest neighbor atoms in a 2.5-ms timescale. The low-temperature atomic ordering may have been caused by the enhancement of atom migration via excess vacancies introduced by high-energy electron irradiation. In conclusion, we have demonstrated that time-resolved electron imaging can directly reveal rapid spatiotemporal fluctuations.

The authors wish to thank Mr. S. Takakuwa, Mr. A. Ohsaki, Mr. Y. Wagatsuma, Dr. S. Ohta, and Mr. M. Ohsaki of JEOL Ltd for their support using the UHVEM. KS acknowledges Professor Emeritus H. Mori of Osaka University for invaluable comments. This study was partially supported by JSPS KAKENHI Grant Numbers JP26286021 and JP16K13640.

[1]P. Andreazza, V. Pierron-Bohnes, F. Tournus, C. Andreazza-Vignolle, and V. Dupuis, Surf. Sci. Rep. **70**, 188 (2015).
[2]K. Sato, T. J. Konno, and Y. Hirotsu, Adv. Imaging Electron Phys. **170**, 165 (2012).
[3]K. Sato, B. Bian, T. Hanada, and Y. Hirotsu, Scr. Mater. **44**, 1389 (2001).
[4]D. Alloyeau, C. Langlois, C. Ricolleau, Y. Le Bouar, and A. Loiseau, Nanotechnology **18**, 375301 (2007).
[5]A. Kovács, K. Sato, V. K. Lazarov, P. L. Galindo, T. J. Konno, and Y. Hirotsu, Phys. Rev. Lett. **103**, 115703 (2009).
[6]K. Sato, A. Kovács, and Y. Hirotsu, Thin Solid Films **519**, 3305 (2011).
[7]A. Chamberod, J. Laugier, and J. M. Penisson, J. Magn. Magn. Mater. **10**, 139 (1979).
[8]E. M. Schulson, J. Nucl. Mater. **83**, 239 (1979).
[9]R. Zee and P. Wilkes, Philos. Mag. A **42**, 463 (1980).
[10]M. Z. Hameed, R. E. Smallman, and M. H. Loretto, Philos. Mag. A **46**, 707 (1982).
[11]S. Banerjee, K. Urban, and M. Wilkens, Acta Metall. **32**, 299 (1984).
[12]S. Banerjee and K. Urban, Phys. Status. Solidi A **81**, 145 (1984).
[13]K. B. Reuter, D. B. Williams, and J. L. Golstein, Metall. Mater. Trans. A **20**, 711 (1989).
[14]K. Sato, T. Kosaka, and T. J. Konno, J. Ceram. Soc. Jpn. **122**, 317 (2014).
[15]K. Sato, K. Yanajima, and T. J. Konno, Philos. Mag. Lett. **92**, 408 (2012).
[16]N. Blanc, F. Tournus, V. Dupuis, and T. Epicier, Phys. Rev. B **83**, 092403 (2011).
[17]I. Jenčič, M. W. Bench, I. M. Robertson, and M. A. Kirk, J. Appl. Phys. **78**, 974 (1995).
[18]B. Bian, K. Sato, Y. Hirotsu, and A. Makino, Appl. Phys. Lett. **75**, 3686 (1999).
[19]F. Tournus, K. Sato, T. Epicier, T. J. Konno, and V. Dupuis, Phys. Rev. Lett. **110**, 055501 (2013).
[20]Y. Iijima, O. Taguchi, and K. Hirano, Trans. Jpn. Inst. Met. **21**, 366 (1980).
[21]R. O. Simmons and R. W. Balluffi, Phys. Rev. **129**, 1533 (1963).
[22]R. A. Johnson, Phys. Rev. **152**, 629 (1966).
[23]U. Köster and J. Meinhardt, Mater. Sci. Eng. A **178**, 271 (1994).
[24]K. Urban, Phys. Status. Solidi A **56**, 157 (1979).
[25]P. Jung, R. L. Chapkin, H. J. Fenzl, K. Reichelt, and P. Wombacher, Phys. Rev. B **8**, 553 (1973).
[26]M. W. Thompson, *Defects and Radiation Damage in Metals* (Cambridge University Press, Cambridge, 1969).
[27]J. W. Corbett, *Electron Radiation Damage in Semiconductors and Metals* (Academic Press, New York, 1966).